ISSN 0915-633X

NATIONAL INSTITUTE FOR FUSION SCIENCE

Nonequilibria in Thermal Emission from Supernova Remnants

K. Masai

(Received – Nov. 4, 1993)

NIFS-264 Dec. 1993

RESEARCH REPORT
NIFS Series

NAGOYA, JAPAN

NONEQUILIBRIA IN THERMAL EMISSION FROM SUPERNOVA REMNANTS

Kuniaki MASAI

Service d'Astrophysique, CEN Saclay, 91191 Gif-sur-Yvette Cedex, France

and

National Institute for Fusion Science, Nagoya 464-01, Japan

Submitted to *Astrophys. J.*

Keywords: collisionless shock wave, supernove remnant, nonequipartition, nonequilibrium ionization, line emission

ABSTRACT

Nonequipartition between the electron and the ion temperatures, and nonequilibrium ionization are discussed in view of thermal X-ray emission from young supernova remnants (SNRs). For electron heating due to Coulomb collisions with ions in the postshock region, an analytical solution is derived for the electron temperature under the adiabatic condition. By Taylor expansion of the solution, we obtain the electron temperature as a function of the electron density, time, and the shock velocity or the shock temperature T_s. With equipartition time t_{Eq}, the solution shows that the electron temperature increases to be $\approx 0.1T_s$ and $0.3T_s$ in $10^{-3}t_{Eq}$ and $10^{-2}t_{Eq}$, respectively. The result is applied to the self-similar solutions for SNRs in the adiabatic phase, i.e., the free expansion phase and the Sedov phase. For SNRs expanding into a uniform density medium, our results predict much slower variation of the electron temperature than the case of full equipartition within the shock. We show the electron temperature plateau on the shocked matter of an SNR, and give analytical expressions of the electron temperature and the resultant free-free luminosity. In the free expansion phase, the electron temperatures of the reverse- and the blast-shocked matter are close to each other in comparison with the case of full equipartition, and their ratio is nearly constant for the ejecta envelope steepness. This results in a larger difference in the free-free luminosities of the two shocks than the case of full equipartition. Ionization processes are discussed in the framework of eigen-value problem to find the key matrix element which is a pivot of the transformation and gives the characteristic time constant. The ionization time $\approx 10^{12}n_e^{-1}$ s for the electron density n_e, and has no systematic dependence either on the electron temperature or the atomic number. The emission from the shocked matter can scale as $n_e t$, but its superposition on a t-old SNR expanding into a uniform density medium may be represented by a lower value than $n_e t$ expected from the ambient matter density and the age. Also the effect of the nonequilibria on the level populations is discussed in view of line emission processes. While innershell ionization followed by fluorescence lines is important in compression waves, radiative recombination followed by cascade lines is important in rarefaction waves. The rarefaction occurs and adiabatically cools the shocked matter rapidly when the shock wave breaks out of the dense circumstellar matter into the rarefied ambient medium.

Subject headings: nebulae: supernova remnants - shock waves - interstellar: matter - plasmas - X-rays: sources - radiation mechanisms

I. INTRODUCTION

Thermal X-ray emission has been one of powerful probes for supernova remnants (SNRs), since the shocks due to interaction of supernova (SN) ejecta with the circumstellar matter and the interstellar matter heat the matter up to the temperature of order of 10^7 K (for reviews of recent X-ray observations, e.g., Aschenbach 1985; Bleeker 1990). X-ray emission of most of shell-type SNRs without stellar source is due to thermal emission from shock heated plasmas, and the spectra of most of the shell-type young SNRs exhibit strong X-ray emission lines indicating a thermal origin (Bleeker 1990). While the X-ray spectra are illustrated with the aid of a number of specific examples, the time scales required for temperature and ionization equilibration are an important aspect to consider in modeling (Bleeker 1990; see also Aschenbach 1985). At least in the young SNRs, the plasma is still ionizing and nonequilibrium effects in the ionization balance are important (Bleeker 1990).

Free-free continuum temperatures obtained from X-ray observations of young SNRs indicate that electrons are heated to several keV (Aschenbach 1985; Bleeker 1990), which is much higher than the electron temperature in the case of no equipartition at all. Therefore, the assumption $T_e \approx T_i$ is not grossly in error (Bleeker 1990) and has been adopted in some spectral analyses of SNRs (see Aschenbach 1985; Bleeker 1990). On the other hand, by analysis of optical spectra of Blamer-dominated SNRs, Smith et al. (1991) show that the intensity ratios do not correspond to either of two extreme cases of no equipartition at all, i.e., $kT_{i,e} = (3/16) m_{i,e} V_s^2$, or complete equipartition, $T_e = T_i$, where $T_{i,e}$ and $m_{i,e}$ are the ion and electron temperatures and masses, respectively, and V_s is the shock velocity.

McKee (1974) gives arguments that collisionless shock with high Mach number could equilibrate the electron and the ion temperatures by plasma instabilities or turbulences. Cargill and Papadopoulos (1988; see also references therein) demonstrate that ion acoustic instability in quasi-perpendicular shocks can increase the electron temperature by a factor of 10^3 with the Alfvén Mach number $M_A \approx 10^2$. Without such mechanisms working on electrons within the shock, electrons must be heated from the initial energy $\approx (3/16) m_e V_s^2$ to $\approx$ keV in the postshock region mainly through Coulomb collisions with ions of the initial energy $\approx (3/16) m_i V_s^2$.

Hence, our interest is how long time is required not for full equipartition but for heating electrons up to $\approx$ keV with Coulomb collisions, and how the time scale and the electron temperature depend on the quantities of the shock. As for nonequilibrium ionization, how the ionization time scale is determined, and what emission processes become important under nonequilibrium conditions. In the present paper, we discuss these questions related to shock heating. Our aim is at clarifying these two processes underlying in the study of SNRs (Aschenbach 1985; Bleeker 1990). As to nonequipartition, we consider only Coulomb collisions in the postshock region for electron heating, because we intend to provide a starting point for the theoretical and observational studies to follow up and propose another

mechanism additionally. For the above purpose, we derive the physical quantities in analytical way with help of some idealized assumptions.

In the following section, electron heating due to Coulomb collisions in the postshock region is discussed. As an example, we apply the result to the self-similar solutions for SNRs in the adiabatic phase in § II b) and c). In § III a) we discuss the ionization process to derive the characteristic time scale for equilibrium. The influence of nonequilibrium ionization on the line emission is discussed in § III b). The atomic data are based on the work by Mewe and his colleagues (e.g., Mewe, Gronenshild & van den Oord 1985 and references therein), Arnaud & Rothenflug (1985), and on IPP/NIFS-AM publications by T. Kato and her colleagues at Institute of Plasma physics, Nagoya University and National Institute for Fusion Science.

II. ELECTRON HEATING

a) Equipartition of Thermal Energy

Without electron heating at the shock front, the shock results in the higher temperature of ions than that of electrons, because the equipartition through Coulomb collisions within the same species can be reached faster than the collisions between electrons and ions. Then, the electrons are heated in the postshock region by transferring the thermal energy of ions through Coulomb collisions. The shock with the velocity V_s can raise the temperature of particles at the shock front to be

$$kT_s = \frac{2(\gamma - 1)}{(\gamma + 1)^2} \mu m_H V_s^2 = \frac{3}{16} \mu m_H V_s^2 \ , \qquad (1)$$

where k, γ, and μ are the Boltzmann constant, the specific heat, the mean molecular weight to hydrogen mass m_H, respectively, and the last expression is attained for ideal gas with $\gamma = 5/3$. Normalizing to T_s, we define the dimensionless temperatures, $\theta_e \equiv T_e/T_s$ and $\theta_i \equiv T_i/T_s$, where T_e and T_i are the temperatures of electrons and ions, respectively. Then the equipartition time between electrons and ions can be expressed as (Spitzer 1962)

$$t_{Eeq} = 5.87 \frac{A_e^{1/2}}{\varepsilon n_e \ln\Lambda} T_s^{3/2} (\theta_e + \varepsilon\theta_i)^{3/2} \ \text{s}, \qquad (2)$$

where n_e is the electron density, A_e the electron mass in units of amu, ε the mass ratio of electron to ion, and $\ln\Lambda$ is the Coulomb logarithm. Hereafter, c.g.s. units are used if not specifically mentioned.

When the electron temperature is not very far from the ion temperature, or $T_e \gg \varepsilon T_i$ in eq. (2), we have $t_{Eeq} \propto T_e^{3/2}$ as a function of the electron temperature. Then the relaxation time is independent of the *test* particle velocity and depends on the lighter, more rapidly moving *field* particle (Spitzer 1978). Under the shock condition of SNRs without pre-heating due to electron thermal conduction or a collective mode associated with the magnetic field, the ion temperature can be rapidly raised to $\approx 2T_s$, but the electron temperature $\approx \varepsilon T_s$ at the shock front. Introducing the time t_s defined by the shock condition T_s or V_s, we rewrite eq. (2) as

$$t_{Eeq} \equiv t_s (\theta_e + \varepsilon\theta_i)^{3/2} \ , \qquad (2')$$

where

$$t_s = 2.5\text{x}10^2 \frac{T_s^{3/2}}{n_e \ln\Lambda} \ \text{s}$$

$$= 2.7\text{x}10^{-11} \frac{\mu^{3/2}}{n_e \ln\Lambda} V_s^3 \ \text{s} \ . \qquad (3)$$

With dimensionless time scale defined as $\tau \equiv t/t_s$, the equipartition process can be described by the following equations,

$$\frac{d\theta_e}{d\tau} = (\theta_i - \theta_e)(\theta_e + \varepsilon\theta_i)^{-3/2} \ , \qquad (4a)$$

$$\frac{d\theta_i}{d\tau} = (\theta_e - \theta_i)(\theta_e + \varepsilon\theta_i)^{-3/2} \ , \qquad (4b)$$

$$\theta_e + \theta_i = 2 \ . \qquad (4c)$$

Eq. 4(c) assures the entropy conservation with charge neutrality through the process in the specific volume. Cooling due to inelastic collisions is ignored. The matter being shocked may be presumed to be a plasma in which hydrogen is fully ionized. Excitation losses escaping through radiation is not important in the early phase of SNR evolutions. An analytical solution of eqs. (4a-c) is:

$$\tau(x) = \left[\frac{1}{3} x^3 + (1+\varepsilon)\, x + \frac{1}{2} (1+\varepsilon)^{3/2} \ln \left| \frac{x - (1+\varepsilon)^{1/2}}{x + (1+\varepsilon)^{1/2}} \right| \right]_x^{x_0} , \qquad (5)$$

with

$$x \equiv \left[(1-\varepsilon)\theta_e + 2\varepsilon \right]^{1/2} ,$$

where $x_0 \approx (3\varepsilon-\varepsilon^2)^{1/2}$ is the initial value corresponding to the initial electron temperature $\approx \varepsilon T_s$ at $\tau = t = 0$. Since $\varepsilon \ll 1$, eq. (5) is approximated to be $\tau \approx (1/2) \ln[(1+x)/(1-x)] - (1/3)x^3 - x$ with $x \gg x_0$ or $T_e \gg \varepsilon T_s$, which can be attained in negligibly short time after the shock, as shown in Fig. 1. With the Taylor expansion about x ($x_0 \ll x \ll 1$) up to the higher order than the fifth, eq. (5) reduces to

$$\tau \approx \frac{1}{5} x^5 \left(1 + \frac{5}{7} x^2 + \frac{5}{9} x^4 + \cdots \right) \approx \frac{1}{5} x^5 \approx \frac{1}{5} \theta_e^{5/2} . \qquad (6)$$

Thus the increase of the electron temperature due to Coulomb collisions with ions is approximately expressed as

$$\theta_e = \frac{T_e}{T_s} \approx (5\tau)^{2/5} \left[1 - \frac{2}{7} (5\tau)^{2/5} \right] \approx (5\tau)^{2/5} = \left(5 \frac{t}{t_s} \right)^{2/5} . \qquad (7)$$

By substituting eq. (3) into the last expression in eq. (7), the electron temperature in the postshock region is obtained as,

$$\begin{aligned} T_e &\approx 0.21\, (\ln\Lambda)^{2/5}\, n_e^{2/5}\, t^{2/5}\, T_s^{2/5} \ \mathrm{K} \\ &\approx 7.3 \times 10^{-5}\, (\mu \ln\Lambda)^{2/5}\, n_e^{2/5}\, t^{2/5}\, V_s^{4/5} \ \mathrm{K} , \end{aligned} \qquad (8)$$

and is found to scale as $(n_e t)^{2/5}$. For the error of the approximation of the first order of 5τ, we can evaluate a correction factor as

$$f_c \equiv 1 - \frac{2}{7} \left(\frac{T_e}{T_s} \right) ,$$

according to the second order approximation in eq. (7). The electron temperature $T_e^{(1)}$ given by eq. (8) can be

replaced by more accurate value of the second order, as $T_e^{(2)} \approx f_c T_e^{(1)}$. This post-correction is useful also for the calculation of the free-free luminosity with $(f_c)^{1/2}$.

Eq. (8) and the last two expressions in eqs. (6) and (7) are valid within $t < 0.1 t_s$, where the deviation from the analytical solution eq. (5) is less than 27%. The approximation up to the second order of $(5\tau)^{2/5}$ in eq. (7) may be applicable for almost whole region of $T_e \gg \varepsilon T_s$; the second order approximation gives a maximum value $T_e/T_s = 7/8$ at $t/t_s = (1/5)\,(7/4)^{5/2} \approx 0.81$. For the illustrative purpose, we plot the electron temperatures given by eq. (7) in Fig. 1, where the solution given by eq. (5) is shown in τ - θ_e space. The approximations are fairly good in a wide range of practical interest in nonequipartition. It should be emphasized that T_e is raised to be $\approx 0.1 T_s$ and $0.3 T_s$, much higher than the initial value $\approx \varepsilon T_s$, only in $t \approx 10^{-3} t_s$ and $t \approx 10^{-2} t_s$, respectively, much shorter than t_s. It still takes a much longer time to achieve complete equipartition.

The process discussed here is a general case of equipartition between electrons and ions through Coulomb collisions. The electrons are heated in the postshock region, and the electron temperature does not affect the shock condition. In a different way from the Taylor-expansion of the analytical solution here, the same result as the last expression in eq. (7) is obtained by Cox & Anderson (1982), and the similar dependence to eq. (8) by Hamilton & Sarazin (1984; see also Hamilton, Sarazin & Chevalier 1983) and by Yoshida & Hanami (1988). By curve fitting to invert the formulation by Itoh (1978), Cox & Anderson (1982) obtain $T_e/T \approx [(5/3)f]^{2/5}$ for $f < 0.1$, where T is the average particle temperature. With the notations here, $T = T_s$ and $f = 3\tau$.

The interaction of the SN ejecta with the ambient matter is adiabatic in the early phase of SNR evolutions, the free expansion phase and the Sedov phase following. Then the result obtained here can be used to calculate the electron temperature which is responsible for the thermal emission. At age t of an SNR, for the matter shocked at time t_0, eq. (8) should be rewritten in a integral form,

$$T_e^{5/2}(t,t_0) \;=\; 0.21^{5/2} \int_{t_0}^{t} \ln\Lambda(t')\; n_e(t')\; T_s(t')\; \mathrm{d}t' \quad .$$

If the matter shocked at $R(t_0)$ expands to $R(t',t_0)$ at time t', the pressure adiabatically varies as $p = (n_i+n_e)T_s \propto [R(t',t_0)/R(t_0)]^{-5}$. With the shocked matter expanding at a velocity $\approx \delta_{nm}\, \mathrm{d}R(t)/\mathrm{d}t$, where δ_{nm} is a numerical factor, we can integrate the above equation. Introducing a function,

$$g_{nm}^{5/2}(t,t_0) \equiv (1-\delta_{nm})^{-5}\,(t_0/t)^{1+\alpha(1-m/\beta)} \int_1^{t/t_0} \left[1+\frac{\delta_{nm}}{1-\delta_{nm}}\,(t'/t_0)^{\alpha/\beta}\right]^{-5} \mathrm{d}(t'/t_0) \ ,$$

we can write the result, as

$$T_e(t,t_0) \ = \ T_e(t)\ g_{nm}(t,t_0) \ . \qquad (8')$$

Here $T_e(t)$ represents the electron temperature given by eq. (8) with the quantities at time t, and $\alpha = -2(3-m)/(n-m)$ and $\beta = -2(3-m)/(n-3)$ are defined by $T_s \propto t^{\alpha}$ and $T_s \propto R^{\beta}$, where R is the SNR radius; accordingly SNR expands as $R \propto t^{\alpha/\beta} \propto t^{(n-3)/(n-m)}$. n and m are defined by $\rho_{ej} \propto r^{-n}$ and $\rho_{am} \propto r^{-m}$ for the density ρ_{ej} of the ejecta envelope and ρ_{am} of the ambient matter in the self-similar analysis discussed in § II b). The Sedov solution is out of physical meaning of the ejecta structure defined by n, but is formally referred to $n = 5$ and $m = 0$. The electron temperature observed from the SNR, the superposition of $T_e(t,t_0)$ over the shocked matter ($0 < t_0 < t$) can be replaced by the superposition of $g_{nm}(t,t_0)$ with $T_e(t)$. It should be noted that $t_0/t = 0$ corresponds not to the SNR center but to the contact interface between the ejecta and the ambient matter, yet it is out of meaning for the Sedov solution, and $t_0/t = 1$ to the present shock front. Fig. 2 shows $g_{nm}(t,t_0)$ for the blast-shocked matter with $\delta_{nm} = 3/4$, where the contact interface is located at $\delta_{nm}\,R(t)$. Also for the reverse shocked matter in the free expansion phase, $g_{nm}(t,t_0)$ gives the similar profile inward the reverse shock front from the contact interface. As demonstrated in Fig. 2, g_{nm} has a plateau with its value around unity. The existence of the T_e plateau is explained for the Sedov solution by Cox & Anderson (1982; see also Itoh 1978) in a different formulation. The above behavior of g_{nm} allows the electron temperature of an SNR at age t to be given primarily by eq. (8) with the quantities at t. Therefore, we put $g_{nm} = 1$ in the following self-similar analysis. The structure or the more accurate value of T_e can be referred to eq. (8') as well as f_c.

b) Free Expansion Phase

The outer part of the density profile of the ejecta envelope can be approximated by a steep power-law in radius (Jones, Smith & Straka 1981; Chevalier & Soker 1989). If the density distribution of the ambient matter is

approximated also by a power-law, the interaction can be described by self-similar solutions (Chevalier 1982a). The density distribution is assumed as $\rho_{ej} = (r/tU_c)^{-n}t^3$ for the ejecta envelope (Chevalier 1982a) and $\rho_{am} = 1.4m_H n_0(r/R_0)^{-m}$ with relative helium abundance to hydrogen $n_{He}/n_H \approx 0.1$ for the ambient matter at a distance r to the center of SN, where U_c is a constant and n_0 is the preshock number density of hydrogen at a distance R_0. The self-similar analysis is valid for $n > 5$ and $m < 3$ (Chevalier 1982a). If the progenitor is surrounded by its past stellar wind, we may have $1.4n_0R_0^2 = (\dot{M}/4\pi m_H V_w) \approx 3.0\text{x}10^{36}\ (\dot{M}/10^{-6}\ \mathrm{M_\odot\ yr^{-1}})\ (V_w/10\ \mathrm{km\ s^{-1}})^{-1}\ \mathrm{cm^{-1}}$ with the mass loss rate $\dot{M}$ and the wind velocity V_w. We assume $n_e/n_H \approx 1.2$ for the electron density in the postshock region. For simplicity we ignore the shell thickness compared to the shell radius. Then, the shell radius is given by (Chevalier 1982b)

$$R = \left[\frac{(3\text{-}m)(4\text{-}m)\ U_c^n}{(n\text{-}3)(n\text{-}4)\ m_H}\right]^{1/(n-m)} (1.4n_0R_0^m)^{-1/(n-m)}\ t^{(n-3)/(n-m)}$$

$$\approx 2.5\text{x}10^{18}\left(\frac{U_c}{3\text{x}10^9}\right) n_0^{-1/9}\left(\frac{t}{10^2\mathrm{yr}}\right)^{2/3}\ \mathrm{cm}\ , \qquad (9)$$

where the last expression is the case of $n = 9$ and $m = 0$, as an example. The self-similar analysis also gives the ratios of the quantities of the reverse shock to the blast shock (Chevalier 1982b),

$$\frac{M_r}{M_b} = \frac{n\text{-}4}{4\text{-}m}\ , \qquad (10a)$$

$$\frac{\rho_r}{\rho_b} = \frac{(n\text{-}3)\ (n\text{-}4)}{(4\text{-}m)\ (3\text{-}m)}\ , \qquad (10b)$$

and

$$\frac{T_{sr}}{T_{sb}} = \left(\frac{3\text{-}m}{n\text{-}3}\right)^2\ , \qquad (10c)$$

where M_r and M_b are the mass taken into the shell from the ejecta envelope and the ambient matter, respectively by the reverse and the blast shocks. Hereafter, the quantities of the reverse shock and the blast shock are denoted by the subscript r and b, respectively. In the case of $m = 0$, $M_r > M_b$ for $n > 8$, $\rho_r > \rho_b$ for $n > 7$, and $T_r < T_b$ for $n > 6$. In the case of $m = 2$, $M_r > M_b$ for $n > 6$, $\rho_r > \rho_b$ and $T_r < T_b$.

Eq. (10c) gives the ratio of the shock temperatures. To calculate the emission from the SNR shell, we obtain the electron temperature by using the relation $T_e \propto \rho^{2/5} T_s^{2/5}$ given by eq. (8), as

$$\frac{T_{er}}{T_{eb}} = \left(\frac{\mu_r \ln\Lambda_r}{\mu_b \ln\Lambda_b}\right)^{2/5} \left[\frac{(n\text{-}4)(3\text{-}m)}{(n\text{-}3)(4\text{-}m)}\right]^{2/5} \approx \left[\frac{(n\text{-}4)(3\text{-}m)}{(n\text{-}3)(4\text{-}m)}\right]^{2/5} , \tag{11}$$

with

$$T_{eb} = 1.2\text{x}10^{-4} (\mu \ln\Lambda)^{2/5} \left(\frac{n\text{-}3}{n\text{-}m}\right)^{4/5} \left[\frac{(3\text{-}m)(4\text{-}m)\, U_c^n}{(n\text{-}3)(n\text{-}4)\, m_H}\right]^{2(2\text{-}m)/5(n\text{-}m)} (1.4 n_0 R_0^m)^{2(n\text{-}2)/5(n\text{-}m)}\, t^{2(2\text{-}m)(n\text{-}3)/5(n\text{-}m)\text{-}2/5}$$

$$\approx 2.7\text{x}10^7 \left(\frac{\mu}{0.61}\right)^{2/5} \left(\frac{\ln\Lambda}{33}\right)^{2/5} \left(\frac{U_c}{3\text{x}10^9}\right)^{4/5} n_0^{14/45} \left(\frac{t}{10^2 \text{yr}}\right)^{2/15} \text{K} , \tag{12}$$

where the last expression in eq. (12) is the case for $n = 9$ and $m = 0$, and the electron temperature of the reverse shock is $2.2\text{x}10^7$ K. Fig. 3 shows the ratios of the electron temperature and the shock temperature of the reverse shock to those of the blast shock. The electron temperature observed from an SNR is likely between T_{eb} and T_{er}, as discussed later. For the same parameters, eqs. (1) and (10c) give $T_{sb} = (3/16)\,(\mu m_H/k)\,(\mathrm{d}R/\mathrm{d}t)^2 \approx 3.7\text{x}10^8$ K and $T_{sr} \approx 9.4\text{x}10^7$ K, which are responsible for the emission if $T_e = T_i$ is established at the shock front. By using these shock temperatures, the correction factors are estimated as $f_{cb} \approx 0.98$ and $f_{cr} \approx 0.93$ for more accurate values of T_{eb} and T_{er} than given by eqs. (12) and (11). In the free expansion phase, the first order approximation may be enough to obtain the electron temperature and the free-free luminosity as mentioned later.

The shock temperature decreases with the age as $T_s \propto (R/t)^2 \propto t^{2(3-m)/(n-m)}$. In the case of $m = 2$, the electron temperature decreases as $T_e \propto t^{2/5}$ independently of n. However, in the case of $m = 0$, the electron temperature increases for $n > 6$, as $T_e \propto t^{2(n-6)/5n}$. Using eqs. (9) and (12), we can find the relations of the electron temperature to the SNR shell radius R and its expansion velocity $\mathrm{d}R/\mathrm{d}t$, as

$$T_{eb} = 1.2\text{x}10^{-4} (\mu \ln\Lambda)^{2/5} \left(\frac{n\text{-}3}{n\text{-}m}\right)^{4/5} \left[\frac{(3\text{-}m)(4\text{-}m)\, U_c^n}{(n\text{-}3)(n\text{-}4)\, m_H}\right]^{2/5(n\text{-}3)} (1.4 n_0 R_0^m)^{2/5\text{-}2/5(n\text{-}3)}\, R^{2(2\text{-}m)/5\text{-}2(n\text{-}m)/5(n\text{-}3)} \text{ K}$$

$$= 1.2\times10^{-4}\,(\mu \ln\Lambda)^{2/5}\left(\frac{n-3}{n-m}\right)^{2/5+2(1-m)(n-3)/5(3-m)}\left[\frac{(3-m)(4-m)\,U_c^n}{(n-3)(n-4)\,m_H}\right]^{2(1-m)/5(3-m)}$$
$$(1.4 n_0 R_0^m)^{4/5(3-m)}\left(\frac{dR}{dt}\right)^{2/5-2(1-m)(n-3)/5(3-m)}\ \mathrm{K}\ . \qquad (13)$$

If full equipartition is established, $T_e = T_s \propto (dR/dt)^2 \propto R^{-2(3-m)/(n-3)}$. With $T \propto t^{\alpha}$ and $T \propto R^{\beta}$, the power α and β are plotted in Figs. 4 (a) and (b), respectively, for n = 6-12 and m = 0 and 2, and for the Sedov solution discussed in § II c).

In the case of $m = 0$ (also in the Sedov phase) T_e approaches T_s with the age t of an SNR, since T_s is higher and decreases faster than T_e. However, when SN is surrounded by its stellar wind ($m = 2$), T_e decreases faster than T_s for $n > 7$, as seen in Figs. 4 (a) and (b). This tendency is more remarkable with larger n. For example, for $n = 12$ and $m = 2$, just after the explosion as early as $t < 11\ [(U_c/3\times10^9)^{-4}\,(\dot{M}/10^{-6}\ \mathrm{M}_\odot\ \mathrm{yr}^{-1})\,(V_w/10\ \mathrm{km\ s}^{-1})^{-1}]^3$ sec, T_e given by eq. (12) would be larger than T_s. Of course, it is not true but means that the density there is high enough to equilibrate the electron and the ion temperatures, i.e., $T_e \approx T_i \approx T_s$. Since the circumstellar density decreases rapidly as R^{-2}, T_e is being left behind T_s soon. Although the self-similar analysis here is not applicable for the early interaction near the progenitor radius (see Chevalier 1982b), the above behavior of T_e suggests a possibility that the shocked matter with $m = 2$ turns to be recombining, as discussed in § III b).

As shown in eq. (12), in SNRs of age ≈ a few 10^2 yr, the electron temperatures of the both shocks are likely > 10^7 K. If the electron temperature is higher than a few 10^7 K, the emission from the SNR shell is dominated by the free-free transitions for $Z \le Z_\odot$, where Z represents the abundance of elements heavier than helium, and $Z_\odot$ is its solar value. The emissions from SNRs are affected by nonequilibrium ionization and the related level populations, as discussed in § III a) and b). However, the free-free emission can be almost free from the nonequilibrium condition, because the transition occurs within the thermal pool of free electrons. The free-free emissivity per n_H^2 is estimated to be ≈ $2.5\times10^{-27} T_e^{1/2}$ erg cm^3 s^{-1} taking into account the helium abundance. With the emission measure $\propto \rho^2(M/\rho)$, we have the ratio of the luminosities due to free-free emission as,

$$\frac{L_\tau^{FF}}{L_b^{FF}} = \left[\left(\frac{n-4}{4-m}\right)^{11}\left(\frac{n-3}{3-m}\right)^4\right]^{1/5}\ , \qquad (14)$$

with

$$L_b^{FF} = 2.3\times10^{-28}(\mu \ln\Lambda)^{1/5}\frac{3}{3-m}\left(\frac{n-3}{n-m}\right)^{2/5}\left[\frac{(3-m)(4-m)\,U_c^n}{(n-3)(n-4)\,m_H}\right]^{(17-11m)/5(n-m)}$$
$$(1.4n_0R_0^m)^{(11n-17)/5(n-m)}\,t^{(17-11m)(n-3)/5(n-m)-1/5}$$

$$\approx 3.2\times10^{33}\left(\frac{\mu}{0.61}\right)^{1/5}\left(\frac{\ln\Lambda}{33}\right)^{1/5}\left(\frac{U_c}{3\times10^9}\right)^{17/5}n_0^{82/45}\left(\frac{t}{10^2\mathrm{yr}}\right)^{31/15}\ \mathrm{erg\ s^{-1}}\ , \qquad (15)$$

where the last expression of eq. (15) is the case for $n = 9$ and $m = 0$. If the equipartition is established at the shock front, the luminosity ratio is $L'_r{}^{FF}/L'_b{}^{FF} = [(n-4)/(4-m)]^2$. The correction factors to the first order approximation are $(f_{cb})^{1/2} \approx 0.99$ and $(f_{cr})^{1/2} \approx 0.97$ for the luminosities of the blast shock and the reverse shock, respectively. When the spectrum is observed within a range of photon energy between E_1 and E_2, the free-free luminosity should be corrected as $L^{FF}(E_1,E_2) = L^{FF}\,[\exp(-E_1/kT_e)-\exp(-E_2/kT_e)]$. Thus, eq. (14) is multiplied by $[\exp(-E_1/kT_{er})-\exp(-E_2/kT_{er})]/[\exp(-E_1/kT_{eb})-\exp(-E_2/kT_{eb})]$. In the free expansion phase of SNRs, as suggested by eq. (10b), the density is higher in the reverse shock than in the blast shock for $n > 7$. This means that the equipartition goes faster in the reverse shock than in the blast shock. As discussed in § III a), also ionization scales as $n_e t$ for a given T_e, and goes faster in the reverse shock for $n > 7$.

The electron temperature of the blast-shocked matter is higher than that of the reverse-shocked matter, as shown in Fig. 3, though the free-free emission is dominated by the latter for $n > 7.5$. Because of higher density in the reverse-shocked ejecta than the blast-shocked ambient matter, the difference in the electron temperature between the two shocked components is reduced to be smaller than the difference in the shock temperature for $n > 7$. As shown in Fig. 3, in both cases of $m = 0$ and 2, the ratio of the electron temperature falls in a narrow range, although the shock temperature distributes in a wide range of order of magnitude with varying n. The electron temperature of the reverse shocked matter is lower than that of the blast shock for any acceptable value of n (> 5), while the shock temperature of the reverse shock is higher than that of the blast shock for $n < 6$ with $m = 0$.

On the other hand, the free-free luminosity ratio spreads in a wider range than that calculated for the shock temperatures. This tendency may be enhanced when the free-free emission is observed in a certain energy range as mentioned before. With increasing n, the free-free emission from the reverse-shocked ejecta envelope dominates more. For the remnants of SNe with smaller n, the two temperature components may be found. However, the difference in the temperature is not very large, as shown in Fig. 3. Using eqs. (10a), (10b) and (11) or (14) and (11), we have a mean electron temperature, as

$$<T_e>_{EM} = \frac{1+\left[\left(\frac{n-4}{4-m}\right)^{12}\left(\frac{n-3}{3-m}\right)^{3}\right]^{1/5}}{1+\left(\frac{n-4}{4-m}\right)^{2}\left(\frac{n-3}{3-m}\right)} T_{eb} \ , \qquad (16)$$

or

$$<T_e>_{FF} = \frac{1+\left[\left(\frac{n-4}{4-m}\right)^{13}\left(\frac{n-3}{3-m}\right)^{2}\right]^{1/5}}{1+\left[\left(\frac{n-4}{4-m}\right)^{11}\left(\frac{n-3}{3-m}\right)^{4}\right]^{1/5}} T_{eb} \ , \qquad (16')$$

where $<T_e>_{EM}$ and $<T_e>_{FF}$ are the electron temperatures emission measure-averaged and the free-free luminosity-averaged, respectively. Eqs. (16) and (16') give $<T_e>_{EM} \approx <T_e>_{FF} \approx 0.87T_{eb}$ for $n = 9$ and $m = 0$. For the same values of n and m, eq. (11) gives $T_{er} \approx 0.83T_{eb}$. The electron temperature observed may be close to the electron temperature of the reverse shock reflecting its larger emission measure. In ionization equilibria with $Z = Z_\odot$, the X-ray line emissivity can be roughly scaled in proportion to T_e^{-1} in the range of $5\text{x}10^6$ K $< T_e <$ a few 10^7 K, above which free-free emission dominates. If the line emission is taken into account, the luminosity-averaged electron temperature is further close to that of the reverse shock.

c) Sedov Phase

The Chevalier's (1982b) self-similar solutions on which the argument in the last section based are valid after the maximum light through the interaction within the power law section of the density profile of the ejecta (Chevalier 1982a). After the reverse shock reaches the ejecta core of nearly flat density profile, the swept-up mass exceeds the mass of the original SN ejecta and dominates the emission from the SNR. In the limit neglecting the ejecta mass compared to the swept-up mass, i.e., for the expansion from a point, the Sedov solutions (1959) can be applied for the shock propagating outward. Since the dynamics of this phase is still adiabatic, we can use the result in § II a) to obtain the electron temperature.

Under the condition $R^3 \gg 2\text{x}10^{56}\,(M_0/M_\odot)\,n_0^{-1}$ cm^3 with the ejecta mass M_0, we have the radius of the SNR shell from the Sedov solution, as

$$R = \left(\frac{1.53E_0}{1.4m_H}\right)^{1/5} n_0^{-1/5}\, t^{2/5} \approx 1.5\text{x}10^{19}\left(\frac{E_0}{10^{51}\text{erg}}\right)^{1/5} n_0^{-1/5}\left(\frac{t}{10^3\text{yr}}\right)^{2/5} \text{cm} \ , \qquad (17)$$

where E_0 is the kinetic energy of the SN explosion. As mentioned in § II a), the Sedov solution formally corresponds to the case of $n = 5$ and $m = 0$ of the self-similar solution in § II b) with replacing U_c by $[(1.53/6)E_0]^{1/5}$. Using eq. (8), we can estimate the electron temperature in this phase, as

$$T_e \approx 2.9\text{x}10^7 \left(\frac{\mu}{0.61}\right)^{2/5} \left(\frac{\ln\Lambda}{33}\right)^{2/5} \left(\frac{E_0}{10^{51}\text{erg}}\right)^{4/25} n_0^{6/25} \left(\frac{t}{10^3\text{yr}}\right)^{-2/25} \text{K} \ . \qquad (18)$$

For the same parameters, the shock temperature is obtained as $T_s = (3/16)\ (\mu m_H/k)\ (\text{d}R/\text{d}t)^2 \approx 4.7\text{x}10^7$ K. Thus, we have the correction factor $f_c \approx 0.82$ and a more accurate value of the electron temperature than in eqs. (18), as $T_e \approx 2.4\text{x}10^7$ K; the electron temperature reaches about half T_s only by Coulomb collisions.

The electron temperature can be rewritten in terms of the SNR radius R or the expansion velocity $\text{d}R/\text{d}t$, as

$$T_e \approx 3.8\ (\mu \ln\Lambda)^{2/5} \left(\frac{E_0\, n_0}{R}\right)^{1/5} \text{K}$$
$$\approx 0.11\ (\mu \ln\Lambda)^{2/5} \left(E_0\, n_0^2 \frac{\text{d}R}{\text{d}t}\right)^{2/15} \text{K} \ . \qquad (19)$$

Eq. (19) suggests a much slower decrease of the electron temperature with time or the expansion than in the case of $T_e = T_i = T_s \propto (\text{d}R/\text{d}t)^2 \propto t^{-6/5} \propto R^{-3}$, as seen in Figs.4 (a) and (b). This difference may be detectable by observations to examine the argument in § II a) and the full equipartition hypothesis. Eqs. (13) and (19) predict little variation (small $|\alpha|$ and $|\beta|$) in the electron temperature with expanding the SNR through the free expansion phase and the Sedov phase. In addition, in the free expansion phase, α and β do not depend so much on n in comparison with the case of $T_e = T_i$. These characteristics may be favorable for detecting the difference mentioned above.

Using eq. (18), the free-free luminosity in the Sedov phase is estimated as

$$L^{FF} \approx 7.0\text{x}10^{35} \left(\frac{\mu}{0.61}\right)^{1/5} \left(\frac{\ln\Lambda}{33}\right)^{1/5} \left(\frac{E_0}{10^{51}\text{erg}}\right)^{17/25} n_0^{38/25} \left(\frac{t}{10^3\text{yr}}\right)^{29/25} \text{erg s}^{-1} \ . \qquad (20)$$

Here the correction factor to eq. (20) is $(f_c)^{1/2} \approx 0.91$. In the Sedov phase, the correction factors for the electron temperature and the resultant free-free emission become larger than those in the free expansion phase, yet the error is still within 20% in the electron temperature on account of $t < 0.1 t_s$.

III. IONIZATION

a) ionization Time Scale

When the electron temperature is lower than 10^7 K with ionization equilibria and $Z \geq Z_\odot$, the emission from the plasma is dominated by the line emission. If the plasma is ionizing, the line emission can dominate up to higher temperatures. Nonequilibrium ionization affects 2γ-decay and free-bound emission as well as line emission. The collisional ionization rate equation for the element of atomic number Z can be written in a form

$$\frac{\mathrm{d}}{\mathrm{d}\, n_e t}\mathbf{n} = \mathsf{F}\,\mathbf{n} = \begin{pmatrix} -S_0 & \alpha_0 & & & & & \\ S_0 & -(S_1+\alpha_1) & \alpha_2 & & & 0 & \\ & S_1 & -(S_2+\alpha_2) & \alpha_3 & & & \\ & & \cdots & \cdots & \cdots & & \\ & & & S_{Z-1} & -(S_Z+\alpha_Z) & \alpha_{Z+1} & \\ & 0 & & & \cdots & \cdots & \cdots \\ & & & & & S_{Z-1} & -\alpha_Z \end{pmatrix} \begin{pmatrix} n_0 \\ n_1 \\ n_2 \\ \vdots \\ n_Z \\ \vdots \\ n_Z \end{pmatrix}, \qquad (21)$$

where S_z and α_z represent the rate coefficients for ionization and recombination from ion of charge z to charge $z+1$ and z-1, respectively, $\mathbf{n}$ is the ionization state vector, and F is a (Z+1)x(Z+1) matrix to be tri-diagonal when multiple ionization or the Auger transition is ignored. F is a function of the electron temperature through the rate coefficients. At a given temperature to determine F, the ion j specified by $S_{j-1} > \alpha_j$ and $S_j < \alpha_{j+1}$ is to be the most abundant in the equilibrium or $n_e t \to \infty$. When $\mathsf{F}(T_e) \approx$ constant, the solution of eq. (21) can be approximately obtained as

$$\mathbf{n}(n_e t) = \exp(n_e t\, \mathsf{F})\, \mathbf{n}_0 = \mathsf{P}\left[\exp(n_e t \lambda_z)\right] \mathsf{P}^{-1}\, \mathbf{n}_0 \ , \qquad (22)$$

where $\mathbf{n}_0$ is the initial value of the ionization state, $[\exp(n_e t \lambda_z)]$ is the diagonal matrix, and $\mathsf{P} = (\mathbf{P}_0, \mathbf{P}_1, \mathbf{P}_2, \ldots, \mathbf{P}_z, \ldots, \mathbf{P}_Z)$ is the matrix to diagonalize F with the eigen column vector $\mathbf{P}_z$ and the eigen value λ_z, as discussed by Masai (1984).

The components of the vector $\mathbf{n}$ represent the fractional ion abundances, which are normalized as $\sum n_z = 1$, i.e., the vector $\mathbf{n}$ is non-orthogonalized. This restraint assures the existence of non-trivial solution given by $\det \mathsf{F} = 0$

or the equilibrium solution for $d\mathbf{n}/d(n_e t) = \mathbf{0}$, and also characterizes the time scale for relaxation. Because of the non-independence, the time required for ionization equilibrium should not be defined for each ionic state n_z but for the vector $\mathbf{n}$, a complete set of ion abundances; $(n_e S_z)^{-1}$ gives the time when the ion z is abundant but has nothing to do with relaxation. An eigen value is zero and all others are negative; as readily seen from eq. (22), all the terms with the negative eigen values vanish at infinite time, and the equilibrium solution is expressed in terms of the zero eigen value.

The characteristic time scale for eq. (21) to realize the ionization equilibrium can be determined by the matrix F, as suggested from the exponential argument in eq. (22). Because of $\det \mathsf{F} = 0$ or the existence of a zero eigen value, however, F^{-1} cannot be defined to be a time constant. Instead, with the zeroth order approximation, we can have the time constant in eq. (21) to be the harmonic mean of the diagonal elements f_{zz} of the matrix F, as

$$n_e t_{leq} \approx \sum_{z=0}^{Z} |f_{zz}|^{-1} = \sum_{z=0}^{Z} (S_z+\alpha_z)^{-1} \ . \qquad (23)$$

Since a diagonal element is outstanding in the harmonic mean, we can approximate eq. (23) as

$$n_e t_{leq} \approx [\min\{(S_z+\alpha_z)\}]^{-1} = [(S_z+\alpha_z)_{\min\{|S_z-\alpha_z|\}}]^{-1} \approx 10^{12} \text{ cm}^{-3} \text{ s} \ , \qquad (23')$$

where $\min\{x_z\}$ represents the minimum among the elements x_z of $z = 0$ to Z, and $(S_z+\alpha_z)_{\min\{|S_z-\alpha_z|\}}$ is the absolute value of the diagonal element that gives the minimum difference between S_z and α_z (Masai 1993).

The zero eigen value is associated with this element, i.e. $\lambda_k = 0$ when $|f_{kk}| = (S_k+\alpha_k)$ is the diagonal element of the minimum absolute value. The ion k is specified by the relation $S_{k-1} > \alpha_{k+1}$ and $S_k < \alpha_{k+2}$, and is a pivot of the transformation in eq. (21). Hence, at a given electron temperature, the ionization time is $\approx (S_k+\alpha_k)^{-1}$ with $S_{k-1} > \alpha_{k+1}$ and $S_k < \alpha_{k+2}$ or with $\lambda_k = 0$, independently of the ionic state. The ion j to be the most abundant at $n_e t \to \infty$ is likely coincident with the ion k discussed here. This is not always the case, for example, when the ion k is Li-like which is sandwiched by more stable ions.

In practice, $(S_k+\alpha_k)^{-1}$ has no systematic dependence either on the electron temperature or the element Z. The last expression in eq. (23') comes from the following result of atomic processes. S_z is an increasing function of the

electron temperature and α_z is a decreasing function except for the region where dielectronic recombination dominates. For each ionic state, these two functions should cross at a certain electron temperature with $S_z \approx \alpha_z \approx 10^{-11}$-$10^{-13}$ cm^3 s^{-1}, where the ionization and recombination are balanced. Varying the electron temperature, we have Z points in total corresponding to the ionic states which are abundant, or more exactly the pivots in eq. (21). All these points are around 10^{-12} cm^3 s^{-1} in scale of the rate coefficients. One may get this behavior and the ionization time $n_e t_{Ieq} \approx 10^{12}$ cm^{-3} s in an empirical way of computations for nonequilibrium ionization.

The emission from a plasma is determined by the energies in the electron thermal pool and in the ionization state, as discussed in § III b). The electron temperature rises in proportion to $(n_e t)^{2/5}$ in the postshock region if only Coulomb collisions are important. Since also the matrix F is a function of $n_e t$ through T_e, the emission from the shocked matter can be scaled with $n_e t$. The ionization progresses following the increase in the electron temperature, and must start with a low electron temperature. When T_e varies, eq. (22) is rewritten and can be approximated for $|\mathbf{n}| = (\Sigma n_z^2)^{1/2} \approx$ constant and $n_e t \gg 0$, as

$$\mathbf{n}(n_e t) = \exp\left(\int_0^t n_e \mathsf{F}\, dt'\right) \mathbf{n}_0 \approx \exp(n_e t\, \mathsf{F}(n_e t))\, \mathbf{n}_0 \ , \qquad (22')$$

where $\mathsf{F}(n_e t)$ is the matrix determined by the present electron temperature $T_e(n_e t)$. In other words, except for the very beginning, the ionization state reached does not depend very much on the history of the electron temperature. $n_e t_{Ieq}$ is nearly comparable to $n_e t_{Eeq}$ and much longer than the electron-electron relaxation time, and has no systematic dependence on the electron temperature. Hence, the approximation by eq. (22') may be useful with $T_e \approx$ constant and the initial ionization state $\mathbf{n}_0$ at $\approx \varepsilon T_s \ll T_e$ or simply the neutral value.

Actually, in the adiabatic phase of SNR, the electron temperatures given by eqs. (11) and (12), or eq. (18), do not vary very much with the age, as seen from small $|\alpha|$ in Fig. 4 (a). For $6 < n < 12$ shown in Fig. 4(a), in the free expansion phase T_e decreases as $T_e \propto t^{2/5}$ for $m = 2$ and increases slower than $T_e \propto t^{1/5}$ for $m = 0$, while T_s decreases faster than $T_s \propto t^{1/5}$ for $m = 2$ and faster than $T_s \propto t^{1/2}$ for $m = 0$. In the Sedov phase $T_e \propto t^{2/25}$, while $T_s \propto t^{6/5}$. These behaviors of the electron temperature support the above argument and scaling the emission from

SNRs with $\eta = n_e t$ being an independent valuable. Hence, the X-ray line emission from SNRs can be represented by a couple of parameters (T_e, η).

Using the results in § II b) and c), the parameter η to indicate the deviation from ionization equilibrium is expressed for the blast shock, as

$$\eta_b = 3.4\left[\frac{(3-m)(4-m)\,U_c^n}{(n-3)(n-4)\,m_H}\right]^{-m/(n-m)} (1.4 n_0 R_0^m)^{n/(n-m)}\, t^{1-m(n-3)/(n-m)}$$

$$\approx 1.5\text{x}10^{11}\, n_0 \left(\frac{t}{10^3 \text{yr}}\right) \text{cm}^{-3}\,\text{s}, \qquad (24)$$

where the last expression is the case of $m = 0$. For the reverse shock η_r is obtained from eq. (10b), as $\eta_r = (\rho_f/\rho_b)\eta_b$, which is $(5/2)\eta_b$ for $n = 9$ and $m = 0$. The Sedov solution can be referred to $m = 0$. Eq. (24) is compared with the equilibrium value $\eta_{leq} \equiv n_e t_{leq} \approx 10^{12}$ cm^{-3} s. At age t, for the matter shocked at t_0, η can be rewritten as

$$\eta(t,t_0) = \int_{t_0}^{t} n_e(t')\mathrm{d}t' = \eta(t)\, h_{nm}(t,t_0)\ , \qquad (24')$$

where $\eta(t)$ represents the product at t, given by eq. (24), and $h_{nm}(t,t_0)$ is written as

$$h_{nm}(t,t_0) \equiv (1-\delta_{nm})^{-3}\,(t_0/t)^{1-\alpha m/\beta} \int_1^{t/t_0} \left[1 + \frac{\delta_{nm}}{1-\delta_{nm}}\,(t'/t_0)^{\alpha/\beta}\right]^{-3} \mathrm{d}(t'/t_0)\ .$$

The function $h_{nm}(t,t_0)$ with $\delta_{nm} = 3/4$ is shown in Fig. 5 for the blast-shocked matter in the same manner as Fig. 2. In contrast to the plateau of g_{nm} for T_e, h_{nm} varies in a wide range. Single-η modeling may not be good to reproduce SNR spectra. In addition, for $m = 0$, h_{nm} gives values considerably below unity. This implies that the emission from t-old SNR is represented by a h_{nm} times smaller value than the present product $n_e t$ given by eq. (24). The analysis of observed spectra may estimate the density or the age at its wrong value, as $(n_0 t)_{obs} \approx h_{nm}\, n_0 t$, lower than the real one.

b) Line Emission

When a plasma is near ionization equilibrium, direct excitation from the ground state plays a dominant role in line emission processes. Here direct excitation means excitation by electron impact directly to outer bound electrons. The satellite lines following dielectronic recombination are enhanced at around ionization equilibria at lower temperatures than the lines due to direct excitation; since the free electron capture goes with resonant excitation of a bound electron into the doubly excited state, the resultant line emission has similar characteristics to excitation rather than recombination. Also the satellite lines due to innershell excitation can contribute in the regime from equilibria toward ionizing. These three processes can account for the line emission almost entirely around ionization equilibria. Then, the energy distributed into the ionization state, which is an internal degree of freedom, is balanced with the energy contained in the electron thermal pool.

In a strongly ionizing condition, the energy of free electrons is much higher than that in the ionization state, and is enough to ionize innershell bound electrons. This process is followed by either electron transitions or fluorescence line emission to stabilize the highly excited state. Into the vacancy produced by innershell ionization, the probability of E1 (electric dipole) radiative transition is approximately proportional to Z^4, while the electron transition (Auger transition) probability does not vary with Z very much. Therefore, the branching ratio for the line emission, the fluorescence yield, can be scaled as $Z^4/(Z^4+C_A)$ with a constant $C_A \approx 10^6$ representing the Auger transition. Therefore, the fluorescence line emission is important for ionizing high Z species like iron. The yield is nearly constant over the ionic states except for the case of innershell ionization of Li-like ion, which results in the forbidden line $1s^2(^1S)$ - $1s2s(^3S)$ of He-like.

In radiative recombination, free electrons are captured predominantly into lower levels. Near ionization equilibria, the probability to capture into a level of principal quantum number n scales as n^{-3} with the hydrogenic approximation. In a recombining condition, the capture probability into higher levels becomes enhanced. With the hydrogenic approximation, the predominant energy levels to capture can be expressed as

$$n < \left(\frac{2I}{3kT_e}\right)^{1/2} \approx \left(\frac{2Z^2 I_H}{3kT_e}\right)^{1/2} ,$$

where I is the ionization potential. In equilibria or ionizing, $n < 2$ and about 80% or more falls directly into the ground state ($n = 1$) to result in the continuum emission. In a strongly recombining condition, n should be larger than 2, and the capture with the continuum emission is followed by cascades to lower levels with the line emission. This process

produces not satellite lines like dielectronic recombination but the lines of the same transitions, thus the same wavelengths, as direct excitation from the ground state by electron impact.

Figs. 6 (a) and (b) show iron Kα line emissivity on T_e - T_z plane, where Kα means all n = 1-2 transitions including satellite lines which fall in the wavelength range from the neutral Fe I Kα to H-like Fe XXVI Lyα (resonance line). T_z is the ionization temperature defined as follows: when the ionization state is approximated by an equilibrium value at an appropriate electron temperature as $\mathbf{n} \approx \mathbf{n}_{eq}(T_e)$, we put $T_z = T_e$ to represent the ionization state in scales of temperature. Accordingly, ionization equilibria, ionizing and recombining conditions are expressed with the relations as $T_z = T_e$, $T_z < T_e$ and $T_z > T_e$, respectively, as indicated in Fig. 6 (a). When a plasma is rapidly heated up from the initial equilibrium state, its trace goes away from $T_e = T_z$ line into the $T_e > T_z$ regime because of the faster increase in T_e than T_z, and approaches $T_e = T_z$ line again with the time scale given by eq. (23'). When a plasma is rapidly cooled, its trace passes through the $T_e < T_z$ regime to approach $T_e = T_z$. With T_z given, higher electron temperature gives higher emissivity in the ionizing regime. This tendency is enhanced in the strongly ionizing regime ($T_e \gg T_z$) due to innershell ionization as well as innershell excitation.

As demonstrated in Fig. 6 (b), innershell ionization - fluorescence and radiative recombination - cascade are important in ionizing and recombining regimes, respectively, and direct excitation and satellite lines due to dielectronic recombination are dominant near equilibria. Satellite lines due to innershell excitation are included in excitation here. The emissivity due to excitation reaches its maximum in the $T_e > T_z$ regime, because this process terminates when T_z is so high as to strip all bound electrons. In radiative recombination from H-like to He-like, the cascades from n > 3 levels enhance more the intercombination $1s^2$ (^{1}S) - 1s2p (^{3}P) 6.67 keV and the forbidden $1s^2$ (^{1}S) - 1s2s (^{3}S) 6.63 keV lines than the resonance line $1s^2$ (^{1}S) - 1s2p (^{1}P) 6.70 keV because of the statistical weights. As a result, the mean energy of the Kα lines is slightly lower in the radiative recombination dominant regime than in the direct excitation dominant regime, as seen in Fig. 6 (a).

The level population affects also the intensity ratios of resonance series (E1-transition) lines such as He-like 1s (^{1}S) - np (^{1}P) and H-like 1s (^{2}S) - np (^{2}P). In the ionizing regime, the 1s-np/1s-2p ratio (n > 2) of the same species (element and ionic state) is larger than that in ionization equilibrium, because $T_e > T_z$ condition enables high-energy direct excitation from the ground state. With increasing the electron temperature, 1s-np transitions of higher n are enhanced. Thus, the ratio can be a measure of the electron temperature, and is a function only of the electron temperature under the coronal population (see § V), which is attained more easily for E1 transitions than non E1 transitions because of the former's larger radiative transition probabilities. In the recombining regime ($T_e < T_z$), the

ratio is also enhanced; but, this is due to a different mechanism from the case of ionizing. The enhancement arises from the cascades following radiative recombination into upper levels, as described before. Then, the 1s-np/1s-2p ratio ($n > 2$) of the same species increases with decreasing the electron temperature. Also in this case, at low densities concerned with SNRs, the ratio is a function only of the electron temperature. Hence, the ratio can be a good measure of the electron temperature free from nonequilibrium ionization, unless the density is so high as to cause collisional transitions from the excited states (see § V). Since the dependence on the electron temperature is different between the ionizing and recombining regimes, observations of more than two ratios of the resonance series lines can distinguish these two cases.

Since the cooling time scale is comparable with the recombination time of an SNR shell, in general, the spectra from young SNRs exhibit ionizing through the adiabatic phase. This is characteristic of compression waves arising from strong shocks. However, when the shock breaks out of a dense clump into the medium of lower density, a rarefaction wave occurs and propagates from the contact interface backward into the dense matter. Such rarefaction waves cool the shocked dense matter with adiabatic expansion much more rapidly than the radiation cooling, when the expansion energy is still high compared to the energy deposited in the electron thermal pool. Then the shocked matter turns rapidly to recombining because of the longer time scale of recombination than electron-electron relaxation; in some cases, ionizing and recombining characteristics coexist. Such a condition of rarefaction can be observed in the early free expansion phase, as in case of the interaction with the circumstellar clumps (Masai & Nomoto 1993) or the Type II SN surrounded by the progenitor's dense stellar wind matter (Itoh & Masai 1989).

V. DISCUSSION AND REMARKS

We demonstrate that Coulomb collisions in the postshock region can raise the electron temperature up to $\approx$ a few keV as observed for SNRs of age of a few 10^2 to 10^3 yr. Such an electron temperature can be reached also by plasma instabilities within the shock (McKee 1974). If equipartition is established at the shock front, the electron temperature deduced from the spectra must satisfy the relation, $T_e = T_s \propto (dR/dt)^2$. Otherwise, $T_e \propto (dR/dt)^{2/5\text{-}2(1\text{-}m)(n\text{-}3)/5(3\text{-}m)}$ may be found being in process of equipartition; T_e is much more weakly dependent on the expansion speed than $T_e = T_s$ in the case of full equipartition. Imaging X-ray telescopes now make available the direct observation of the T_e - expansion law for more than one decade since the Einstein satellite. Also the time evolution of the emission temperature can be investigated by long-term observations. In the free expansion phase with $m = 0$ and $6 < n < 12$ shown in Figs. 4 (a) and (b), the electron temperature predicted increases slower than $T_e \propto t^{1/5} \propto R^{4/15}$,

while the equipartition within the shock predicts the electron temperature decreasing faster than $T_e = T_s \propto t^{1/2} \propto R^{-2/3}$. In the Sedov phase, our calculation and the full equipartition predict, as $T_e \propto t^{2/25} \propto R^{-1/5}$ and $T_e = T_s \propto t^{6/5} \propto R^{-3}$, respectively. In any case of adiabatic expansion into a uniform density medium, our calculation predicts a distinctively smaller change in the electron temperature with evolution of SNR than the case of full equipartition, as seen in Figs. 4 (a) and (b).

In § II b) and c) we apply the result of § II a) to the adiabatic phase of SNRs to demonstrate the density dependence of the equipartition process. Eqs. (9) - (16) are valid for SNRs after the maximum light through the reverse shock propagates within the envelope described by $\rho_{ej} \propto r^n$ (Chevalier 1982a, b), and eqs. (17) - (20) are valid after the swept-up mass much exceeds the ejecta mass. Therefore, the argument from § II b) through c) cannot continue crossing the transient phase. In both cases, one has to recall the validity of eq. (8), i.e., eqs. (11) - (16) and (18) - (20) are valid within $t < 0.1 t_s$, which depends on the density, as given by eq. (3); with the correction factor f_c, one can obtain more accurate numerical coefficients of the second order for these equations, which can be applied up to $\approx 0.8 t_s$ or $T_e \approx 0.9 T_s$. The above condition may be satisfied almost through the adiabatic phase of SNR because the cooling time of the SNR shell is nearly comparable to t_s. SNRs may be influenced by the local structures in the ambient matter. In this case, eq. (7) or (8) may be useful for interpretation.

In the free expansion phase, the free-free luminosity is dominated by that from the reverse-shocked ejecta for $n > 7.5$. The outer ejecta may consist of heavier elements than hydrogen depending on the progenitor, while hydrogen is the majority in the ambient matter. This affects the equipartition in the reverse shocked matter, and the electron temperature ratio given by eq. (11) must be corrected by the ratio of the electron density to the mass density. Also the charge dependence of the free-free emission must be taken into account for obtaining the luminosity, although it does not alter the conclusion that the reverse shock is predominant. One should notice the self-similar analysis discussed here is applicable for the ambient matter monotonically distributed as $\rho \propto r^m$. The interaction of the ejecta with a clumpy matter like the circumstellar ring of SN 1987A does not always give $L_r^{FF} > L_b^{FF}$ even before the reverse shock reaches the ejecta core (e.g., see Masai & Nomoto 1993). When SN is surrounded by its past wind, the solutions with $m = 2$ may be applied. For $n > 7$, just after the explosion $T_e \approx T_s$ is likely attained, and T_e begins to decrease faster than T_s soon, as suggested in § II b). This behavior must come out to recombining emission discussed in § III b), as demonstrated numerically by Itoh & Masai (1989), when the shock breaks out of the circumstellar matter into the rarefied medium. A supersonic stellar wind can form a low-density bobble surrounded by a dense shell (Weaver, McCray & Castor 1977). When SN explodes in such a structure of the stellar wind matter, the interaction can be described by another self-similar solutions (Chevalier & Liang 1989). Then, recombining emission is expected

when the blast shock breaks out of the dense shell.

When electrons are heated in the postshock region with dependence as eq. (8), the shocked matter exhibits a plateau in the electron temperature. In the case of expansion into a uniform density medium ($m = 0$), the free-free emission of an SNR may be represented approximately by a single electron temperature. However, the ionization state of the shocked matter, which is responsible for the line emission, is not represented by a single component of (T_e, η), as discussed in § III a). This suggests that attention must be paid to multi-component ionization state as well as multi-component temperature in the spectral analysis of SNRs. In fact, the X-ray spectra of SNRs are not well represented by single nonequilibrium models, but require at least two components (Aschenbach 1985). If the resonance series lines are resolved for He-like or H-like ions, as discussed in § III b), the 1s-np/1s-2p ratios of the same species can be a good measure of T_e independently of η. The electron temperatures thus obtained are likely diverse but should reflect straightforwardly the environment of each species. The behavior of h_{nm} has to be considered to estimate the product of the ambient matter density and the age. In the case of $m = 0$, even multi-(T_e, η) analysis may estimate the product at a lower value. In particular, the matter near the contact interface ($t_0/t \ll 1$) can exhibit a significantly lower value of η in both the reverse and the blast shocks. This may come out to the diverse η values dependent on the elements, if the ejecta leave a layer structure of the chemical composition.

In Figs. 2 and 5, we demonstrate g_{nm} and h_{nm} for a case of $\delta_{nm} = 3/4$ of the blast-shocked matter. On the other hand, in the argument in § II b), we ignore the thickness of the SNR shell compared to its radius (Chevalier 1982b), and approximate the blast-shock velocity by the shell velocity, as $V_{sb} \approx dR/dt$, to obtain T_s and T_e. Chevalier (1982a) gives the self-similar solutions taking into account the shell structure for the interaction in the free expansion phase. From these solutions and the shell structure of the Sedov solution, δ_{nm} can be determined for each case of n and m. However, the characteristic behaviors of g_{nm} and h_{nm}, discussed in § II a) and III a), are not altered by the acceptable values of δ_{nm}.

Nonequilibrium ionization is discussed in the framework of the atomic collision space. If the element concerned is moving with respect to the electron thermal pool, the effective time for collisions is reduced. One can replace the time t by $t' \equiv (t^{-1}+t_d^{-1})^{-1}$ to extend the argument in § III a) approximately to moving space, with t_d representing the characteristic time of the dynamical motion. This treatment corresponds to the transformation from the Eulerian $\partial/\partial t$ to the Lagrangian D/Dt. Then, the condition to attain the equilibrium is given by $t' > t_{leq} \approx 10^{12} n_e^{-1}$ s. The characteristic time t_d during which the element stays in the thermal pool, may be evaluated as $t_d^{-1} \approx u \nabla \ln T_e$

for the effective velocity u with respective to the thermal pool. When the dynamical motion is so dominant as $t_d < t_{leq}$, the ionization does not reach its equilibrium even at $t \rightarrow \infty$ because of $t' \approx t_d < t_{leq}$, and the ionization state is frozen with $\mathbf{n}(n_e t_d)$. This may allow to probe the dynamical motion relative to the electron thermal pool, when the ionization state stays far from its equilibrium value even after long time satisfying $t > t_{leq}$. Such a situation may be found in spectra of solar flares.

The level population and the resultant line emission processes are affected not only by nonequilibrium ionization as discussed in § III b) but also the electron density which enhances the collisional transitions competing with the radiative decay. In order to treat the level populations as well as the ion abundances, so called collisional-radiative models can be applied in the similar framework to eq. (21), where $n_e t$ is no more independent valuable. However, in the low density plasmas concerned with SNRs, so-called coronal populations can be substantially attained (e.g., Mewe et al. 1985); the ground state is predominantly populated because collisional excitation therefrom is immediately followed by radiative decay. For instance, the density effect appears on the He-like intercombination and forbidden lines at $n_e > 10^{-3}Z^{14}$ cm^{-3}. This is not the case for the X-ray lines from SNRs, and the radiative electron capture in recombining is followed by cascades to lower levels with line emission, as discussed in § III b). It should be noted that the plasma is recombining under the presence of ionizing photons, in a sense of the level population and the line emissivity, even when the recombination is balanced with the total ionization (Masai 1993 and references therein). Then, in photoionized plasmas like accretion matter onto compact stars emitting UV and X-rays, photoionization - fluorescence and radiative recombination - cascade play important roles for K-line emission. Since the population is dominated by radiative recombination - cascade from upper levels, the coronal population is no more a good approximation even at the low density limit.

I am grateful to J. Trümper and B. Aschenbach for discussions and their hospitality at Max-Planck Institute für Extraterrestrische Physik where a part of this work was done. Also to C. Cezarsky, M. Arnaud and their colleagues for their hospitality at Service d'Astrophysique, CEN Saclay. I would like to thank R. McCray for his critical reading the manuscript and useful suggestions.

REFERENCES

Aschenbach, B. 1985, Space Sci. Rev., 40, 447.

Arnaud, M., & Rothenflug, R. 1985, A&A Suppl., 60, 425.

Bleeker, J. A. M. 1990, Adv. Space Res., 10, (2)143.

Cargill, P. J., & Papadopoulos, K. 1988, Ap. J. Lett., 329, L29.

Chevalier, R. A. 1982a, Ap. J., 258, 790.

Chevalier, R. A. 1982b, Ap. J., 259, 302.

Chevalier, R. A., & Soker N. 1989, Ap. J., 341, 867.

Chevalier, R. A., & Liang E. P. 1989, Ap. J., 344, 332.

Cox, D. P., & Anderson, P. R. 1982, Ap. J., 253, 268.

Hamilton, A. J. S., Sarazin, C. L., & Chevalier, R. A. 1983, Ap. J. Suppl., 51, 115.

Hamilton, A. J. S., & Sarazin, C. L. 1984, Ap. J., 284, 601.

Itoh, H., & Masai, K. 1989, MNRAS, 236, 885.

Itoh, H. 1978, PASJ, 30, 489.

Jones, E. M., Smith, B. W., & Straka, W. C. 1981, Ap. J., 249, 185.

Masai, K. 1984, Astrophys. Space Sci. 98, 367.

Masai, K., & Nomoto, K. 1994, Ap. J., in press,

Masai, K. 1993, *Plasma Physics and Controlled Nuclear Fusion - Plasma Astrophysics* (eds. T. D. Guyenne & J. J. Hunt), ESA SP 351, ESTEC, The Netherlands, p. 131.

Mewe, R., Gronenshild, E. H. B. M., & van den Oord H. J. 1985, A&A Suppl., 62, 197.

McKee, C. F. 1974, Ap. J., 188, 335.

Sedov, L. I. 1959, *Similarity and Dimensional Methods in Mechanics*, Academic Press, New York.

Smith, R. C., Kirshner, R. P., Blair W. P., & Winkler, P. F. 1991, Ap. J., 375, 652.

Spitzer, L. 1962, *Physics of Fully Ionized Gases*, Wiley-Interscience, New York.

Spitzer, L. 1978, *Physical Processes in the Interstellar Medium*, Wiley-Interscience, New York.

Weaver, R., McCray, R. & Castor J. 1977, Ap. J., 218, 377.

Yoshida, T., & Hanami, H. 1988, Prog. Theor. Phys., 80, 83.

Figure Captions

Fig. 1 Evolution of the electron temperature $\theta_e = T_e/T_s$ with time $\tau = t/t_s$ due to Coulomb collisions with ions in the postshock region. The solid, broken and dotted lines represent the analytical solution given by eq. (5) and its approximations up to the second order and the first order of $(5\tau)^{2/5}$ given by eq. (7), respectively.

Fig. 2 $g_{nm}(t,t_0)$, which represents the electron temperature at t of the matter shocked at t_0, is plotted for the blast-shocked matter with $\delta_{nm} = 3/4$ (see text). The dotted and solid lines represent the cases of $m = 0$ and $m = 2$, respectively, for $n = 6, 7, 8, 9, 10, 11$ and 12 in the free expansion phase (Chevalier 1982b solution) with the density $\rho_{ej} \propto r^n$ for the ejecta envelope and $\rho_{am} \propto r^m$ for the ambient matter, and the broken line represents the Sedov solution.

Fig. 3 The shock temperature ratio T_{si}/T_{sb} and the electron temperature ratio T_{ei}/T_{eb} of the reverse-shocked ejecta envelope to the blast-shocked ambient matter in the free expansion phase. If $T_e = T_i$ is attained within the shock, T_{si}/T_{sb} (broken lines) represents the ratio of the electron temperature.

Fig. 4 With (a) $T \propto t^{\alpha}$ and (b) $T \propto R^{\beta}$, α and β are plotted for n and m in the free expansion phase and for the Sedov solution, where the Sedov solution is formally referred to $n = 5$ and $m = 0$. SNR expands as $R \propto t^{\alpha/\beta}$. T_e (solid lines) means the prediction for the electron temperature in the present work. Full equipartition within the shock predicts $T_e = T_i = T_s$ (broken lines).

Fig. 5 $h_{nm}(t,t_0)$, which represents the ionization state at t of the matter shocked at t_0, is plotted for the blast-shocked matter in the same manner as in Fig. 2. The dotted and solid lines represent the cases of $m = 0$ and $m = 2$, respectively, for $n = 6, 7, 8, 9, 10, 11$ and 12 in the free expansion phase, and the broken line represents the Sedov solution.

Fig. 6 (a) The iron Kα emissivity (solid lines) and the emissivity-averaged line energy (broken lines) as a function of the electron temperature T_e and the ionization temperature T_z (see text). n = 1-2 transitions including satellites of all ionic states are taken into account. The emissivity is given in units of photons

$cm^3\ s^{-1}$ per n_H^2 with relative iron abundance $n_{Fe}/n_H = 4x10^{-5}$, and its contours are drawn with 0.2 step in the logarithmic scale. The contour of the line energy is linearly stepping. (b) The contribution to iron Kα emissivity is shown for each emission process on the same diagram as (a). The satellite lines due to innershell excitation are included in the lines due to excitation (upper-right).

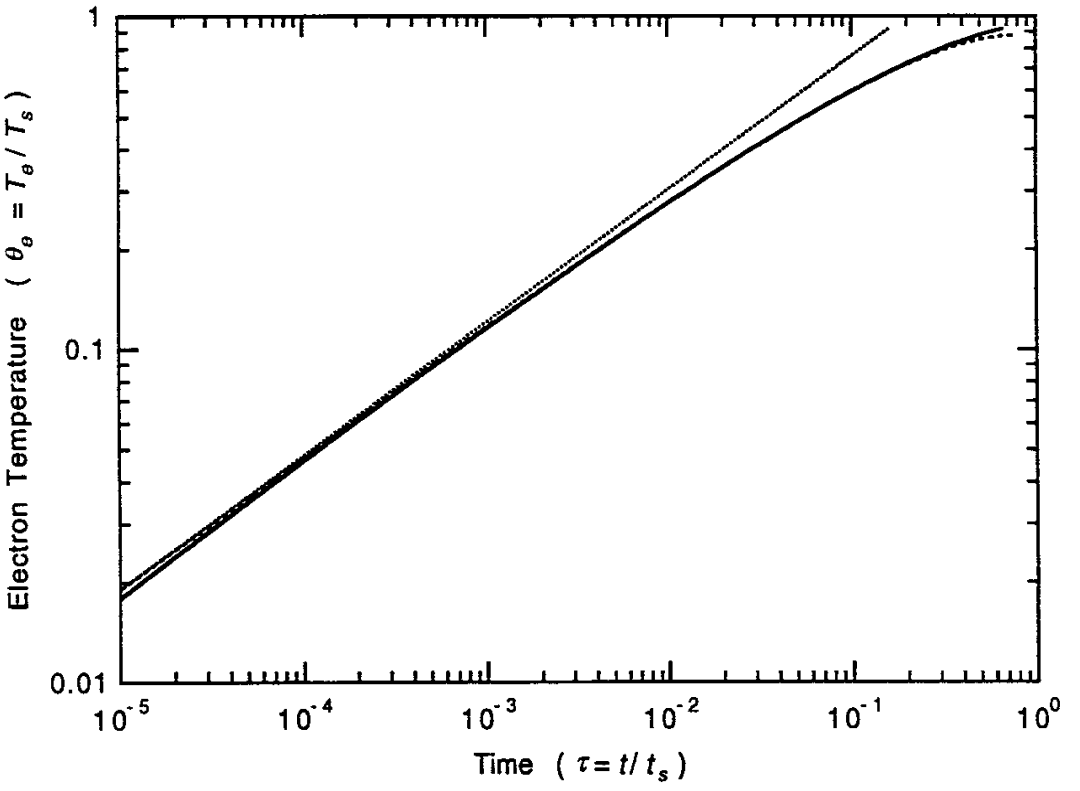
1
0.1
0.01
Electron Temperature ($\theta_e = T_e / T_s$)
10^{-5}
10^{-4}
10^{-3}
10^{-2}
10^{-1}
10^{0}
Time ($\tau = t / t_s$)

Fig. 1

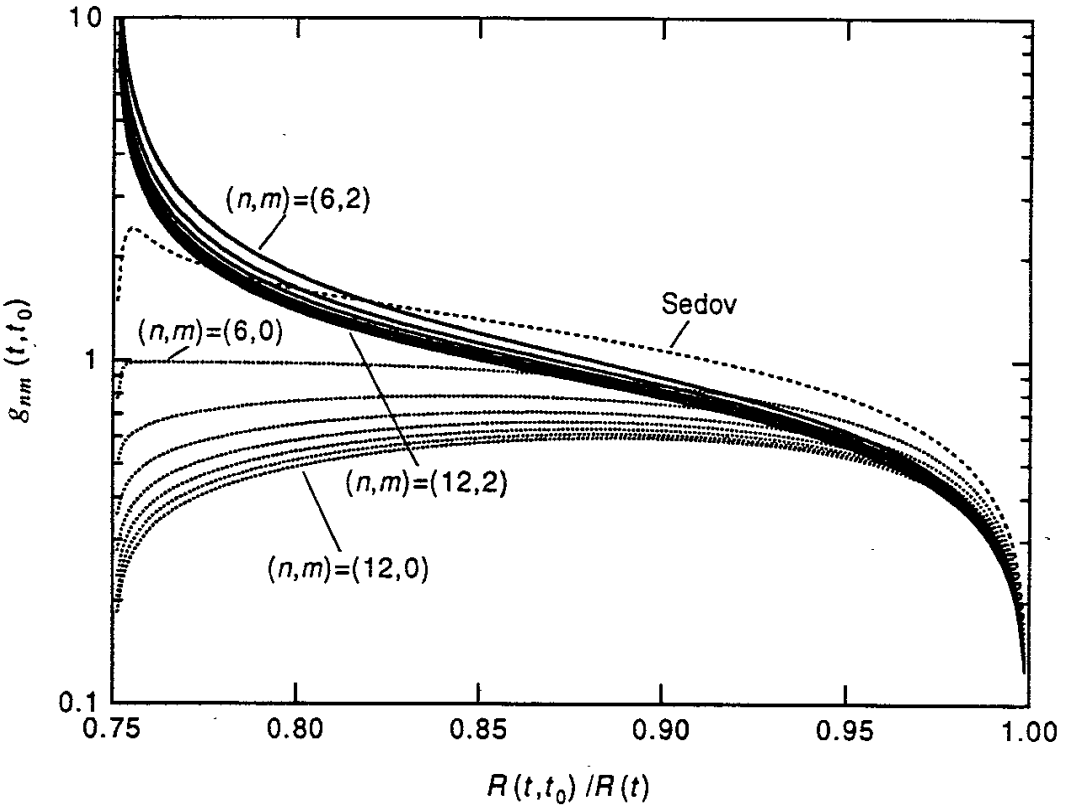
10
1
0.1
0.75
0.80
0.85
0.90
0.95
1.00
$g_{nm}(t,t_0)$
$R(t,t_0)/R(t)$
(n,m)=(6,2)
Sedov
(n,m)=(6,0)
(n,m)=(12,2)
(n,m)=(12,0)

Fig. 2

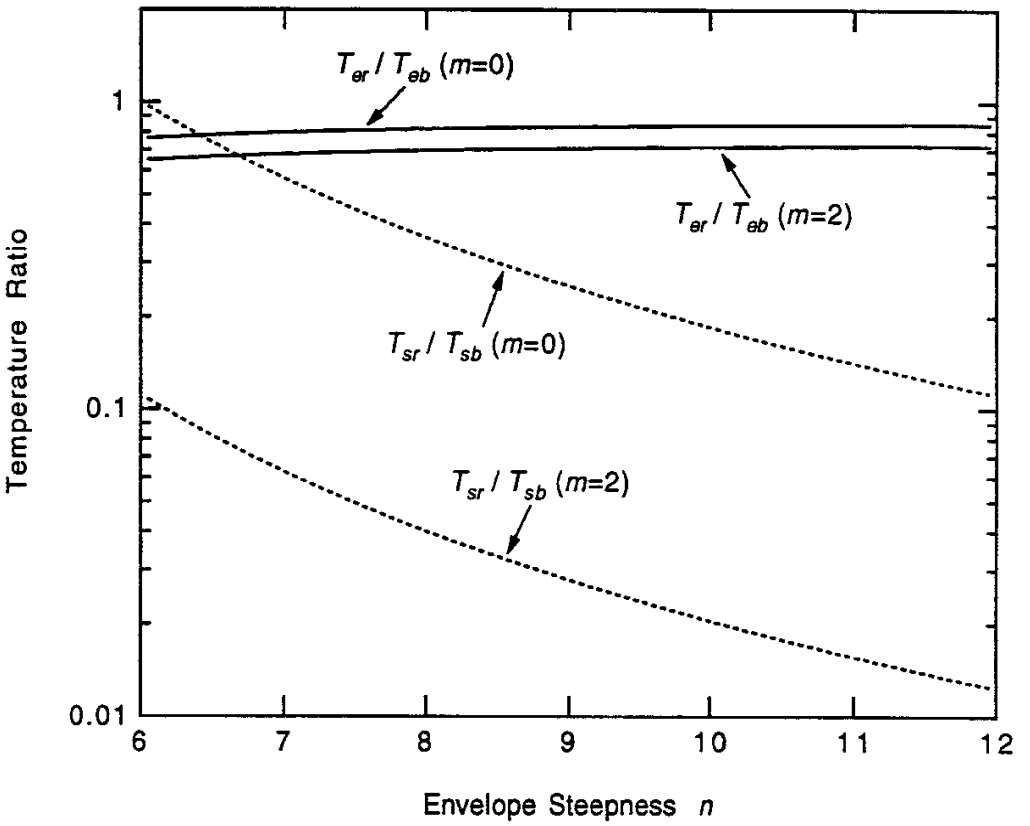
T_{er} / T_{eb} (m=0)
T_{er} / T_{eb} (m=2)
T_{sr} / T_{sb} (m=0)
T_{sr} / T_{sb} (m=2)
Temperature Ratio
1
0.1
0.01
6
7
8
9
10
11
12
Envelope Steepness n

Fig. 3

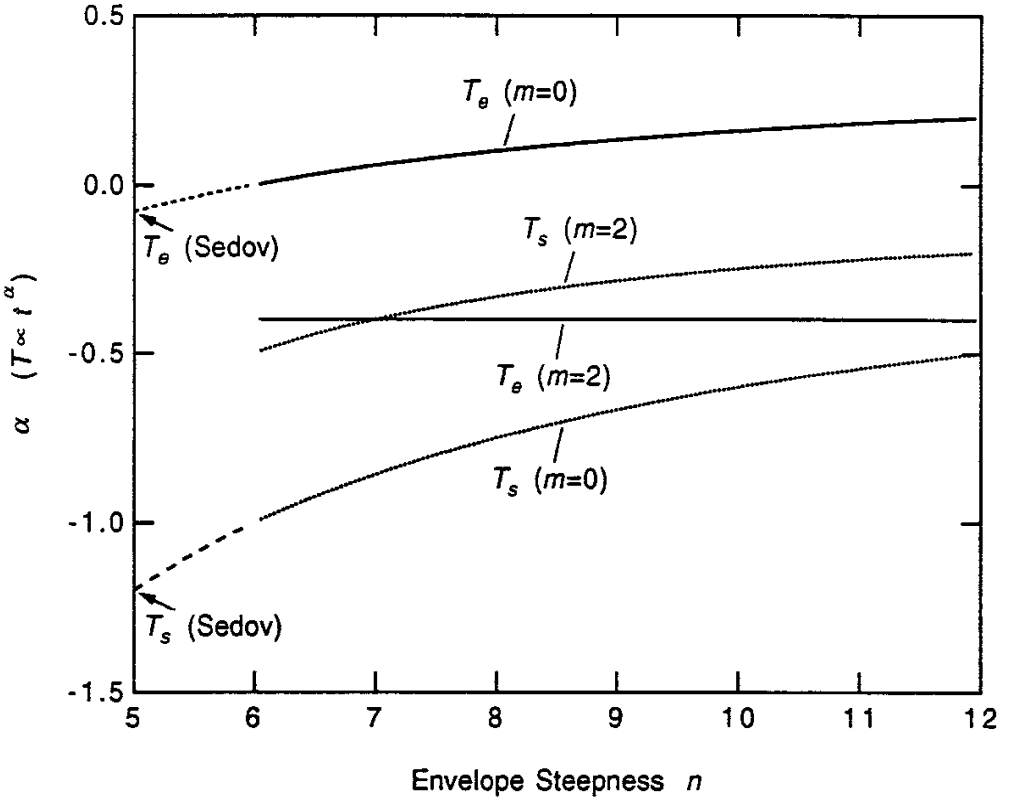
0.5
0.0
-0.5
-1.0
-1.5
5
6
7
8
9
10
11
12
α (T∝t^α)
Envelope Steepness n
T_e (m=0)
T_e (Sedov)
T_s (m=2)
T_e (m=2)
T_s (m=0)
T_s (Sedov)

Fig. 4 (a)

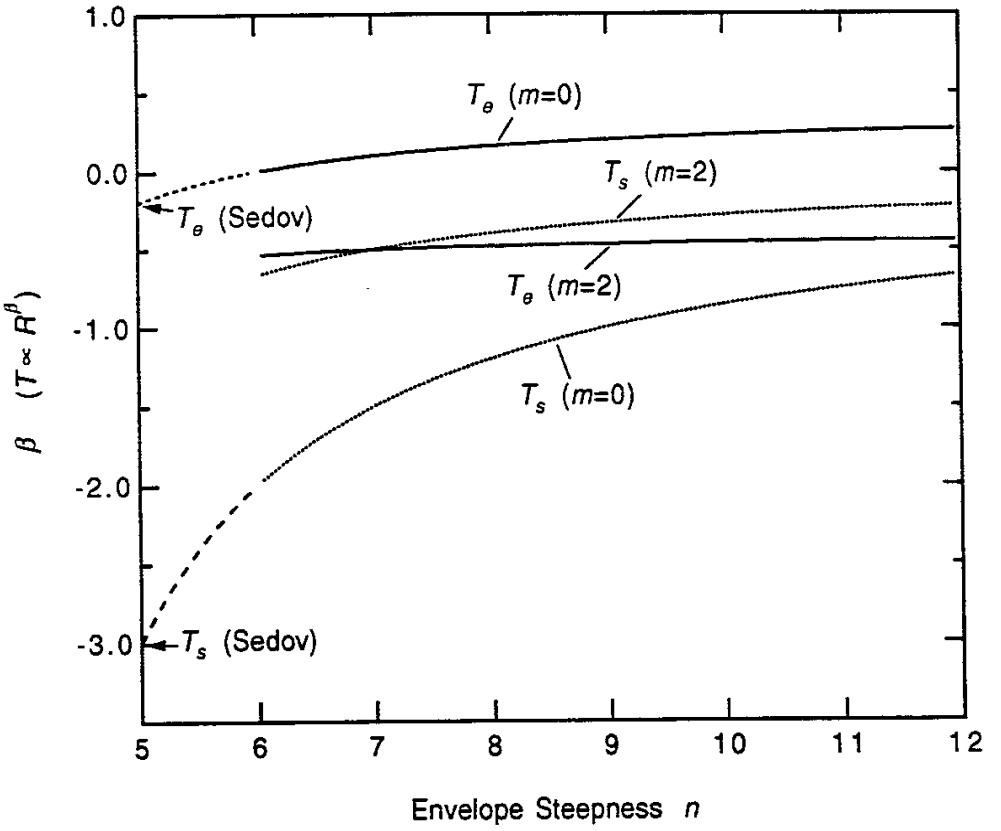
1.0
0.0
-1.0
-2.0
-3.0
β (T∝R^β)
T_e (m=0)
T_s (m=2)
T_e (Sedov)
T_e (m=2)
T_s (m=0)
T_s (Sedov)
5
6
7
8
9
10
11
12
Envelope Steepness n

Fig. 4(b)

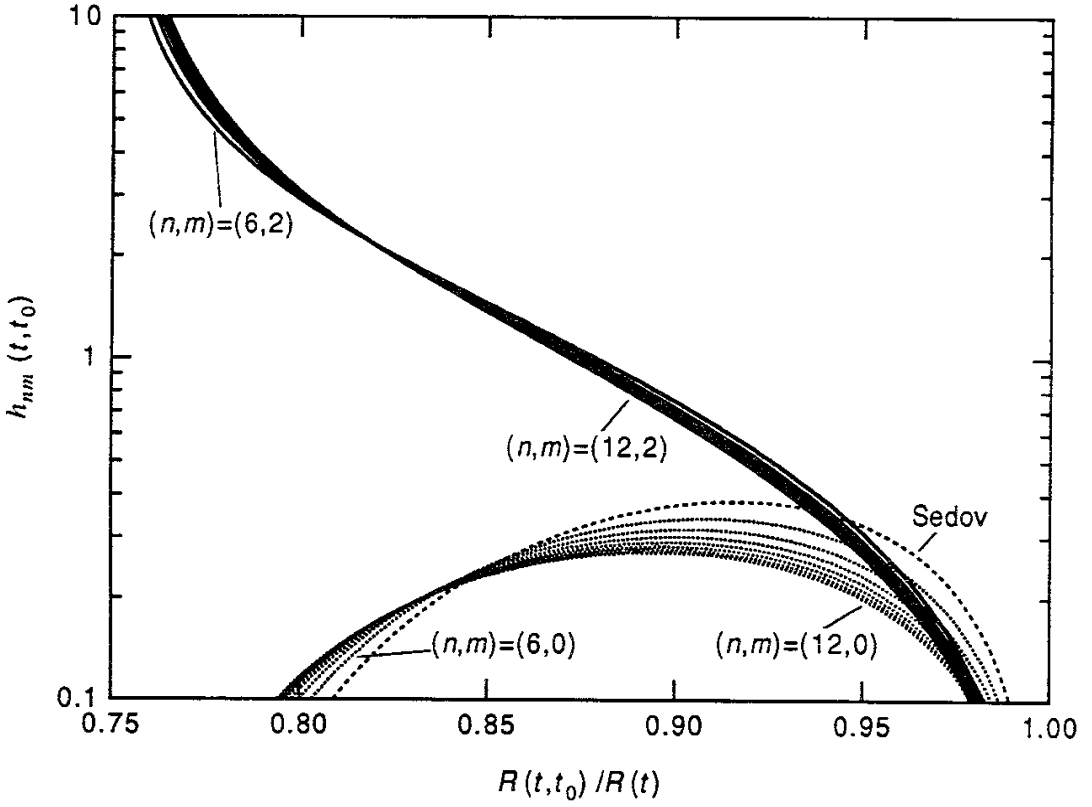
10
1
0.1
0.75
0.80
0.85
0.90
0.95
1.00
$h_{nm}(t,t_0)$
$R(t,t_0)/R(t)$
(n,m)=(6,2)
(n,m)=(12,2)
Sedov
(n,m)=(6,0)
(n,m)=(12,0)

Fig. 5

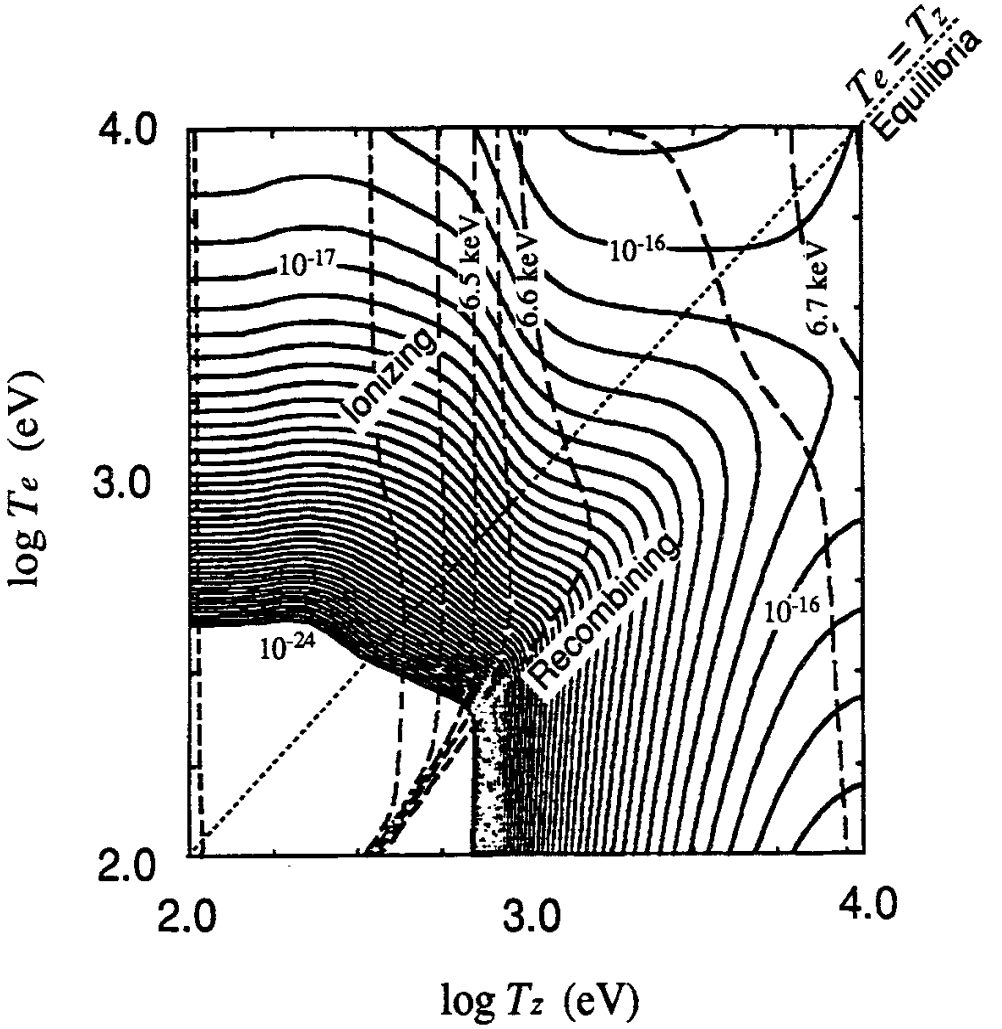
$T_e = T_z$
Equilibria
4.0
3.0
2.0
2.0
3.0
4.0
log T_e (eV)
log T_z (eV)
10^{-17}
10^{-16}
10^{-24}
10^{-16}
6.5 keV
6.6 keV
6.7 keV
Ionizing
Recombining

Fig. 6 (a)

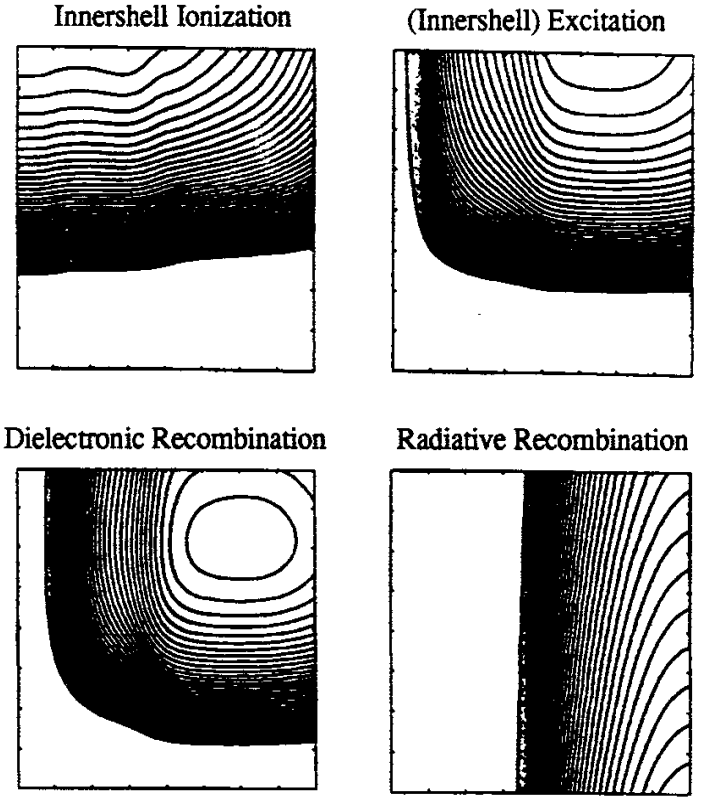
Innershell Ionization
(Innershell) Excitation
Dielectronic Recombination
Radiative Recombination

Fig. 6 (b)

Recent Issues of NIFS Series

NIFS-214 T. Yamagishi, *Effect of Continuous Eigenvalue Spectrum on Plasma Transport in Toroidal Systems*; Mar. 1993

NIFS-215 K. Ida, K. Itoh, S.-I.Itoh, Y. Miura, JFT-2M Group and A. Fukuyama, *Thickness of the Layer of Strong Radial Electric Field in JFT-2M H-mode Plasmas*; Apr. 1993

NIFS-216 M. Yagi, K. Itoh, S.-I. Itoh, A. Fukuyama and M. Azumi, *Analysis of Current Diffusive Ballooning Mode*; Apr. 1993

NIFS-217 J. Guasp, K. Yamazaki and O. Motojima, *Particle Orbit Analysis for LHD Helical Axis Configurations* ; Apr. 1993

NIFS-218 T. Yabe, T. Ito and M. Okazaki, *Holography Machine HORN-1 for Computer-aided Retrieve of Virtual Three-dimensional Image* ; Apr. 1993

NIFS-219 K. Itoh, S.-I. Itoh, A. Fukuyama, M. Yagi and M. Azumi, *Self-sustained Turbulence and L-Mode Confinement in Toroidal Plasmas* ; Apr. 1993

NIFS-220 T. Watari, R. Kumazawa, T. Mutoh, T. Seki, K. Nishimura and F. Shimpo, *Applications of Non-resonant RF Forces to Improvement of Tokamak Reactor Performances Part I: Application of Ponderomotive Force* ; May 1993

NIFS-221 S.-I. Itoh, K. Itoh, and A. Fukuyama, *ELMy-H mode as Limit Cycle and Transient Responses of H-modes in Tokamaks* ; May 1993

NIFS-222 H. Hojo, M. Inutake, M. Ichimura, R. Katsumata and T. Watanabe, *Interchange Stability Criteria for Anisotropic Central-Cell Plasmas in the Tandem Mirror GAMMA 10 ;* May 1993

NIFS-223 K. Itoh, S.-I. Itoh, M. Yagi, A. Fukuyama and M. Azumi, *Theory of Pseudo-Classical Confinement and Transmutation to L-Mode;* May 1993

NIFS-224 M. Tanaka, *HIDENEK: An Implicit Particle Simulation of Kinetic-MHD Phenomena in Three-Dimensional Plasmas;* May 1993

NIFS-225 H. Hojo and T. Hatori, *Bounce Resonance Heating and Transport in a Magnetic Mirror;* May 1993

NIFS-226 S.-I. Iton, K. Itoh, A. Fukuyama, M. Yagi, *Theory of Anomalous Transport in H-Mode Plasmas;* May 1993

NIFS-227 T. Yamagishi, *Anomalous Cross Field Flux in CHS ;* May 1993

NIFS-228 Y. Ohkouchi, S. Sasaki, S. Takamura, T. Kato, *Effective Emission and Ionization Rate Coefficients of Atomic Carbons in Plasmas;* June 1993

NIFS-229 K. Itoh, M. Yagi, A. Fukuyama, S.-I. Itoh and M. Azumi, *Comment on 'A Mean Field Ohm's Law for Collisionless Plasmas;* June 1993

NIFS-230 H. Idei, K. Ida, H. Sanuki, H. Yamada, H. Iguchi, S. Kubo, R. Akiyama, H. Arimoto, M. Fujiwara, M. Hosokawa, K. Matsuoka, S. Morita, K. Nishimura, K. Ohkubo, S. Okamura, S. Sakakibara, C. Takahashi, Y. Takita, K. Tsumori and I. Yamada, *Transition of Radial Electric Field by Electron Cyclotron Heating in Stellarator Plasmas;* June 1993

NIFS-231 H.J. Gardner and K. Ichiguchi, *Free-Boundary Equilibrium Studies for the Large Helical Device,* June 1993

NIFS-232 K. Itoh, S.-I. Itoh, A. Fukuyama, H. Sanuki and M. Yagi, *Confinement Improvement in H-Mode-Like Plasmas in Helical Systems,* June 1993

NIFS-233 R. Horiuchi and T. Sato, *Collisionless Driven Magnetic Reconnection,* June 1993

NIFS-234 K. Itoh, S.-I. Itoh, A. Fukuyama, M. Yagi and M. *Azumi, Prandtl Number of Toroidal Plasmas;* June 1993

NIFS-235 S. Kawata, S. Kato and S. Kiyokawa , *Screening Constants for Plasma;* June 1993

NIFS-236 A. Fujisawa and Y. Hamada, *Theoretical Study of Cylindrical Energy Analyzers for MeV Range Heavy Ion Beam Probes;* July 1993

NIFS-237 N. Ohyabu, A. Sagara, T. Ono, T. Kawamura and O. Motojima, *Carbon Sheet Pumping;* July 1993

NIFS-238 K. Watanabe, T. Sato and Y. Nakayama, *Q-profile Flattening due to Nonlinear Development of Resistive Kink Mode and Ensuing Fast Crash in Sawtooth Oscillations;* July 1993

NIFS-239 N. Ohyabu, T. Watanabe, Hantao Ji, H. Akao, T. Ono, T. Kawamura, K. Yamazaki, K. Akaishi, N. Inoue, A. Komori, Y. Kubota, N. Noda, A. Sagara, H. Suzuki, O. Motojima, M. Fujiwara, A. Iiyoshi, *LHD Helical Divertor;* July 1993

NIFS-240 Y. Miura, F. Okano, N. Suzuki, M. Mori, K. Hoshino, H. Maeda, T. Takizuka, JFT-2M Group, K. Itoh and S.-I. Itoh, *Ion Heat Pulse*

after Sawtooth Crash in the JFT-2M Tokamak; Aug. 1993

NIFS-241 K. Ida, Y.Miura, T. Matsuda, K. Itoh and JFT-2M Group, *Observation of non Diffusive Term of Toroidal Momentum Transport in the JFT-2M Tokamak;* Aug. 1993

NIFS-242 O.J.W.F. Kardaun, S.-I. Itoh, K. Itoh and J.W.P.F. Kardaun, *Discriminant Analysis to Predict the Occurrence of ELMS in H-Mode Discharges;* Aug. 1993

NIFS-243 K. Itoh, S.-I. Itoh, A. Fukuyama, *Modelling of Transport Phenomena;* Sep. 1993

NIFS-244 J. Todoroki, *Averaged Resistive MHD Equations;* Sep. 1993

NIFS-245 M. Tanaka, *The Origin of Collisionless Dissipation in Magnetic Reconnection;* Sep. 1993

NIFS-246 M. Yagi, K. Itoh, S.-I. Itoh, A. Fukuyama and M. Azumi, *Current Diffusive Ballooning Mode in Seecond Stability Region of Tokamaks;* Sep. 1993

NIFS-247 T. Yamagishi, *Trapped Electron Instabilities due to Electron Temperature Gradient and Anomalous Transport;* Oct. 1993

NIFS-248 Y. Kondoh, *Attractors of Dissipative Structure in Three Disspative Fluids;* Oct. 1993

NIFS-249 S. Murakami, M. Okamoto, N. Nakajima, M. Ohnishi, H. Okada, *Monte Carlo Simulation Study of the ICRF Minority Heating in the Large Helical Device;* Oct. 1993

NIFS-250 A. Iiyoshi, H. Momota, O. Motojima, M. Okamoto, S. Sudo, Y. Tomita, S. Yamaguchi, M. Ohnishi, M. Onozuka, C. Uenosono, *Innovative Energy Production in Fusion Reactors;* Oct. 1993

NIFS-251 H. Momota, O. Motojima, M. Okamoto, S. Sudo, Y. Tomita, S. Yamaguchi, A. Iiyoshi, M. Onozuka, M. Ohnishi, C. Uenosono, *Characteristics of D-^{3}He Fueled FRC Reactor: ARTEMIS-L,* Nov. 1993

NIFS-252 Y. Tomita, L.Y. Shu, H. Momota, *Direct Energy Conversion System for D-^{3}He Fusion,* Nov. 1993

NIFS-253 S. Sudo, Y. Tomita, S. Yamaguchi, A. Iiyoshi, H. Momota, O. Motojima,

M. Okamoto, M. Ohnishi, M. Onozuka, C. Uenosono,
Hydrogen Production in Fusion Reactors, Nov. 1993

NIFS-254 S. Yamaguchi, A. Iiyoshi, O. Motojima, M. Okamoto, S. Sudo, M. Ohnishi, M. Onozuka, C. Uenosono,
Direct Energy Conversion of Radiation Energy in Fusion Reactor, Nov. 1993

NIFS-255 S. Sudo, M. Kanno, H. Kaneko, S. Saka, T. Shirai, T. Baba,
Proposed High Speed Pellet Injection System "HIPEL" for Large Helical Device
Nov. 1993

NIFS-256 S. Yamada, H. Chikaraishi, S. Tanahashi, T. Mito, K. Takahata, N. Yanagi, M. Sakamoto, A. Nishimura, O. Motojima, J. Yamamoto, Y. Yonenaga, R. Watanabe,
Improvement of a High Current DC Power Supply System for Testing the Large Scaled Superconducting Cables and Magnets; Nov. 1993

NIFS-257 S. Sasaki, Y. Uesugi, S. Takamura, H. Sanuki, K. Kadota,
Temporal Behavior of the Electron Density Profile During Limiter Biasing in the HYBTOK-II Tokamak; Nov. 1993

NIFS-258 K. Yamazaki, H. Kaneko, S. Yamaguchi, K.Y. Watanabe, Y.Taniguchi, O.Motojima, LHD Group,
Design of Central Control System for Large Helical Device (LHD); Nov. 1993

NIFS-259 K. Yamazaki, H. Kaneko, S. Yamaguchi, K.Y. Watanabe, Y.Taniguchi, O.Motojima, LHD Group,
Design of Central Control System for Large Helical Device (LHD); Nov. 1993

NIFS-260 B.V.Kuteev,
Pellet Ablation in Large Helical Device; Nov. 1993

NIFS-261 K. Yamazaki,
Proposal of "MODULAR HELIOTRON': Advanced Modular Helical System Compatible with Closed Helical Divertor; Nov. 1993

NIFS-262 V.D.Pustovitov,
Some Theoretical Problems of Magnetic Diagnostics in Tokamaks and Stellarators; Dec. 1993

NIFS-263 A. Fujisawa, H. Iguchi, Y. Hamada
A Study of Non-Ideal Focus Properties of 30° Parallel Plate Energy Analyzers; Dec. 1993